

MIT Open Access Articles

*Nanoscale Vector dc Magnetometry via
Ancilla-Assisted Frequency Up-Conversion*

The MIT Faculty has made this article openly available. **Please share** how this access benefits you. Your story matters.

Citation: Liu, Yi-Xiang et al. "Nanoscale Vector dc Magnetometry via Ancilla-Assisted Frequency Up-Conversion." *Physical Review Letters* 122, 10 (March 2019): 100501 © 2019 American Physical Society

As Published: <http://dx.doi.org/10.1103/PhysRevLett.122.100501>

Publisher: American Physical Society

Persistent URL: <http://hdl.handle.net/1721.1/120967>

Version: Final published version: final published article, as it appeared in a journal, conference proceedings, or other formally published context

Terms of Use: Article is made available in accordance with the publisher's policy and may be subject to US copyright law. Please refer to the publisher's site for terms of use.



Nanoscale Vector dc Magnetometry via Ancilla-Assisted Frequency Up-Conversion

Yi-Xiang Liu (刘仪襄)^{1,*}, Ashok Ajoy,^{1,2,*} and Paola Cappellaro^{1,†}

¹Research Laboratory of Electronics and Department of Nuclear Science and Engineering, Massachusetts Institute of Technology, Cambridge, Massachusetts 02139, USA

²Department of Chemistry, University of California Berkeley, and Materials Science Division Lawrence Berkeley National Laboratory, Berkeley, California 94720, USA

 (Received 5 July 2018; published 13 March 2019)

Sensing static magnetic fields with high sensitivity and spatial resolution is critical to many applications in fundamental physics, bioimaging, and materials science. Even more beneficial would be full vector magnetometry with nanoscale spatial resolution. Several versatile magnetometry platforms have emerged over the past decade, such as electronic spins associated with nitrogen vacancy (NV) centers in diamond. Achieving vector magnetometry has, however, often required using an ensemble of sensors or degrading the sensitivity. Here we introduce a hybrid magnetometry platform, consisting of a sensor and an ancillary qubit, that allows vector magnetometry of static fields. While more generally applicable, we demonstrate the method for an electronic NV sensor and a nuclear spin qubit. In particular, sensing transverse fields relies on frequency up-conversion of the dc fields through the ancillary qubit, allowing quantum lock-in detection with low-frequency noise rejection. In combination with the Ramsey detection of longitudinal fields, our frequency up-conversion scheme delivers a sensitive technique for vector dc magnetometry at the nanoscale.

DOI: 10.1103/PhysRevLett.122.100501

Magnetic field sensors have come of age over the past few decades. Particularly compelling are those constructed out of nitrogen vacancy (NV) centers in diamond [1,2], representing a prime example of harnessing spins for *quantum* sensing [3]. The NV center electronic spin is exquisitely sensitive to magnetic fields and has enabled magnetometry at the nanoscale, with sensor footprints spanning a single lattice site. There is particularly wide interest in field sensors responsive “in the dc”—several signals of interest in condensed matter and biological processes, such as the firing of action potentials in single neurons [4–6] arise at low frequencies. Exploiting the NV center for dc magnetometry allows the measurement of these fields at short length scales, potentially opening new tools for probing a diverse set of phenomena including edge currents in topological insulators [7] and quantum wells [8], and spin order in magnetic materials [9].

dc magnetic field sensing is conventionally performed via the Ramsey technique [10], where the sensor evolves freely acquiring a phase under the field to be measured [see Fig. 1(a)]. This method is sensitive to longitudinal fields, whereas the effect of transverse field components are strongly suppressed. The sensor is thus restricted to operate as a scalar magnetometer, precluding extraction of the complete *vector* information of the field to be measured. If such vector magnetometry were indeed possible with a fixed nanoscale sensor, a wealth of additional information could potentially be discerned: for instance, the directionality of an action potential firing, to aid in the mapping of

neuronal networks [4,5], or the reconstruction without gauge assumptions of vector magnetic fields from 2D static and dynamic magnetic textures [11].

In this Letter we introduce and experimentally demonstrate a quantum sensing protocol that achieves vector

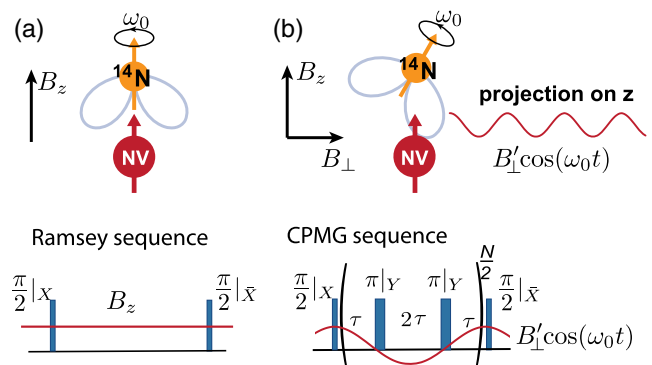


FIG. 1. Vector magnetometry. (a) The magnetic field component B_z along the NV axis can be measured by a Ramsey sequence. Without the transverse field, there is no $S_z I_{\perp}$ interaction (light blue) between the NV ^{14}N nuclear spin and the electronic spin, that only feels a static field. (b) The transverse field modifies the hyperfine coupling, introducing an effective $S_z I_{\perp}$ coupling at the position of the NV. As the nuclear spin precesses at its Larmor frequency ω_0 , the effective field felt by the NV is now an oscillating ac field with amplitude B_{\perp}' proportional to B_{\perp} , that can be measured by a CPMG sequence of N π pulses separated by $2\tau = \pi/\omega_0$.

magnetometry. We combine conventional Ramsey magnetometry with a technique that exploits an ancilla spin to frequency up-convert transverse dc fields to longitudinal ac fields, which can be subsequently detected via quantum lock-in detection [12]. Although transverse dc noise ultimately limits the coherence time, up-conversion aids in rejecting dc longitudinal noise that typically plagues the quantum sensor, enabling much longer interrogation times and high sensitivity transverse field sensing performance [see Fig. 1(b)]. While our protocol is general and directly extendable to atomic magnetometry platforms, we focus our attention on a hybrid NV sensor, employing the electron and ^{14}N nuclear spins collocated at the NV center site. As we demonstrate, the achievable sensitivity for transverse field is on the order of the Ramsey sensitivity to longitudinal fields, and together these measurements enable sensitive, low noise, full vector nanoscale magnetometry with a single point defect sensor.

Conventional dc magnetometry.—We begin our discussion by remarking that the sensitive detection of an external magnetic field by a quantum probe requires strong coupling to the external field γ and good quantum coherence enabling long interrogation time t , since the sensitivity η is $\eta \propto 1/(\gamma\sqrt{t})$ [3]. For simplicity, we consider a generic qubit sensor with Hamiltonian

$$H_0 = \Delta S_z + \gamma(B_z S_z + B_\perp S_\perp), \quad (1)$$

where Δ is the energy (Zeeman splitting) of the qubit and S_\perp is in a direction perpendicular to Z . Our goal is to perform vector magnetometry, that is, determine both B_z and B_\perp , including its azimuthal angle. A magnetic field aligned with the quantum spin probe quantization axis (Z axis) can be detected with good sensitivity since it results in a frequency shift of the probe via the coupling γ . In a Ramsey experiment [see Fig. 1(a)], given an interrogation time τ (bounded by the dephasing time T_2^*), we can extract the external field B_z to be determined from the qubit $m_s = 0$ population:

$$S = \frac{1}{2}[1 + \cos(\gamma B_z \tau)]. \quad (2)$$

Actually, given the Hamiltonian in Eq. (1), the Ramsey experiment will measure a frequency shift $\delta\omega = \sqrt{(\Delta + \gamma B_z)^2 + (\gamma B_\perp)^2} - \Delta$. In principle, we could then also extract the transverse field from Ramsey interferometry. However when Δ is dominant, as typically needed to achieve good control of the qubit sensor, the sensitivity to the transverse field is significantly worse than the Z -field sensitivity. Indeed, expanding $\delta\omega$ to first order in $1/\Delta$ we have,

$$\delta\omega \approx \gamma B_z + \frac{1}{2} \frac{(\gamma B_\perp)^2}{\Delta}.$$

The contribution of B_\perp is quadratic and rescaled by an effective coupling $\gamma_{R^2} = \gamma^2/(2\Delta)$; hence the sensitivity to the transverse field is degraded as $\eta_\perp \propto \sqrt{\Delta}\eta_z$. Indeed, the contribution from the transverse field can be usually neglected (or, in our scheme, subtracted from the frequency shift after being measured).

Transverse magnetometry via frequency up-conversion.— Since we cannot change the coupling strength between the quantum probe and the transverse field, we can act on the allowed interrogation time, by lengthening the coherence time. It has been shown that dynamical decoupling (DD) sequences comprising regularly spaced π pulses can greatly enhance the coherence time of quantum sensors by removing quasistatic noise [13]. The sensor, however, is no longer sensitive to static, dc fields. By mixing the field to be detected with an oscillating bias field, one can, however, achieve frequency up-conversion of the (transverse) dc field, allowing its lock-in detection. We assume the ac bias field adds the term $\omega_{ac} \cos(\omega_0 t) S_\perp$ to Hamiltonian (1). To second order perturbation theory, this gives rise to a time-dependent frequency shift

$$H_{ac} = \frac{\gamma B_\perp \omega_{ac}}{\Delta} \cos(\omega_0 t) S_z. \quad (3)$$

This achieves two goals: first, the frequency shift is linear in the transverse field and is multiplied by an effective coupling $\gamma_{ac} = \gamma \omega_{ac}/\Delta$ that can be made larger than γ_R in the Ramsey scheme; second, because the field is oscillating at ω_0 , we can use DD schemes to detect it, thus achieving longer coherence times, bounded by T_2 and not T_2^* as in the Ramsey sequence. Note that the Z component of the dc field to be measured does not affect the frequency up-conversion process to first order.

We can go one step further and exploit an intrinsic oscillating source for frequency up-conversion, thus avoiding any additional noise that could be introduced by the bias ac field. To achieve frequency up-conversion we exploit the coherent coupling between the qubit probe and an ancillary qubit system. We assume that the quantum probe S is sensitive to the dc signal we want to detect, but the ancillary qubit I does not couple to it (or the coupling is very weak). The sensor-ancilla Hamiltonian is then

$$H = H_0 + \omega_n I_z + H_{hyp}, \quad \text{with} \\ H_{hyp} = A_z S_z I_z + A_\perp (S_x I_x + S_y I_y),$$

H_0 as in Eq. (1), and ω_n the Zeeman energy of the ancillary qubit. The transverse hyperfine interaction $\propto A_\perp$ becomes time dependent in the rotating frame defined by $\omega_0 I_z$, with $\omega_0 = \omega_n - A_z/2$, and plays the same role of the classical bias ac field. To see this, consider that under the assumption $\Delta \gg A_\perp, \gamma B_\perp$, the interaction with transverse field and transverse hyperfine coupling can only drive virtual transitions of the NV spin, due to its larger quantization energy;

when both virtual transitions are present, however, they result in a shift of the NV spin energy, which is equivalent to adding a longitudinal magnetic field. As this is a second order perturbation effect, the energy shift is $\propto B_{\perp}A_{\perp}I_{\perp}/\Delta$, i.e., suppressed by the main NV energy Δ . Effectively, the hyperfine coupling becomes

$$H'_{\text{hyp}} \approx A_z S_z I_z + \frac{\gamma B_{\perp} A_{\perp}}{\Delta} F S_z I_{\perp}, \quad (4)$$

where F is a constant that depends on the nuclear ancilla spin. In the rotating frame defined by $\omega_0 I_z$ the last term becomes time dependent and the qubit sensor effectively sees an ac field $\propto B_{\perp} \cos(\omega_0 t)$ [compare Eq. (3) with Eq. (4)]. The nuclear qubit is thus analogous to an oscillating bias field at a frequency ω_0 set by nature. In the presence of the transverse magnetic field, the sensor couples to this oscillator, up-converting [14,15] the transverse dc field B_{\perp} to a longitudinal ac field at frequency ω_0 [see Fig. 1(b)]. This ac field can now be measured using well-known quantum lock-in techniques, e.g., the CPMG/XY8 protocol [16–18], based on trains of π pulses with pulse spacing set at the effective ac field period [see Fig. 1(b)].

This simple model can be applied to many quantum sensor systems. Here focusing on the NV center, we consider using a nearby nuclear spin as the ancilla, for instance, the ^{14}N nuclear spin intrinsic to every NV center. For this system we have $\Delta = \Delta_0 - \gamma_e B_z$ (where $\Delta_0 = 2\pi \times 2.87$ GHz is the NV zero field splitting, $\gamma_e = 2\pi \times 2.8$ MHz/G is the gyromagnetic ratio of electron and we consider the $m_s = 0, -1$ levels). The frequency ω_0 of the effective ac fields will depend on the spin system considered, for the ^{14}N we have $\omega_0 = Q + \omega_n - (A_z/2)$, where $\omega_n = \gamma_n B_z$ with $\gamma_n = -2\pi \times 0.308$ kHz/G, $A_z = -2\pi \times 2.16$ MHz, and $Q = -2\pi \times 4.95$ MHz [19].

For small B_{\perp} fields, the quantum lock-in CPMG signal at the resonance condition $2\tau = \pi/\omega_0$ [see Fig. 2(a)] is well approximated by [20]

$$S = \frac{1}{2} \left[1 + \cos \left(\frac{\gamma_e B_{\perp} A_{\perp} N}{\omega_0 \Delta} F \right) \right], \quad (5)$$

where N is the number of π pulses. For ^{14}N , $A_{\perp} = -2\pi \times 2.62$ MHz [49] and $F \approx 2.75$, as determined from second order perturbation theory [20]. This signal is especially strong close to the NV center ground state level anticrossing (GSLAC, $B_z \approx 1025$ G), where $\Delta \rightarrow 0$. By fixing the interpulse distance at the resonance condition and changing the number of π pulses, oscillations are observed [see Fig. 2(b)] and B_{\perp} can be extracted from the oscillation frequency using Eq. (5).

Note that while the ^{14}N spin is a natural choice since it is present in every NV center, and provides the added benefit of high robustness to magnetic field fluctuations [20], an ancillary ^{13}C spin in the first few shells [51,52] could provide a wider dynamic range and reduce certain experimental constraints due to its strong hyperfine coupling.

Determination of azimuthal angle.—Ramsey and CPMG experiments reveal the amplitude of the Z component B_z and the transverse component B_{\perp} of the dc field. To perform full vector magnetometry we still need to determine the azimuthal angle of the transverse field. This can be achieved with the help of a reference field \mathbf{B}_r , with fixed direction along X and tunable amplitude. Let ϕ be the angle between \mathbf{B}_{\perp} and \mathbf{B}_r . In the presence of \mathbf{B}_r , the CPMG signal measures the magnitude of the total transverse field $\mathbf{B}_{\text{tot}} = \mathbf{B}_r + \mathbf{B}_{\perp}$,

$$B_{\text{tot}} = \sqrt{|\mathbf{B}_r|^2 + |\mathbf{B}_{\perp}|^2 + 2|\mathbf{B}_r||\mathbf{B}_{\perp}|\cos\phi}, \quad (6)$$

By varying $|\mathbf{B}_r|$ and measuring B_{tot} , we can extract the azimuthal angle ϕ . In principle only two settings of the reference field are needed to extract $|\mathbf{B}_r|$ and ϕ , as we demonstrate (see Ref. [20]) by evaluating the intrinsic field misalignment in our setup.

Theoretical sensitivity bounds.—The shot-noise limited sensitivity η can generally be found from the smallest field δB one could measure at the most sensitive bias point in the total averaging time [53]. Given a finite coherence time T_2 , the sensitivity is optimal for interrogation times $t \propto T_2$ and is determined by the coupling strength to the field to be measured and the interrogation time, $\eta \propto 1/(\gamma\sqrt{T_2})$ [3]. For example, for Ramsey magnetometry of Z fields, the sensitivity is $\eta_Z = 1/(C\gamma\sqrt{T_2^*})$, where C is a factor encapsulating readout inefficiencies. In the frequency-up-conversion lock-in detection method, both the coupling strength and the coherence times are modified, and we obtain $\eta_X = \pi/(2C\gamma_X\sqrt{T_2(\gamma_X)})$, where $\gamma_X \equiv \gamma_e A_{\perp} F/\Delta$. Here T_2 is the coherence time under a DD sequence with interpulse spacing fixed at $2\tau = \pi/\omega_0$, which is generally longer than T_2^* . However, if there is a strong source of transverse dc noise, such as if there is noise embedded in the signal to be measured, T_2 will depend on γ_X and might

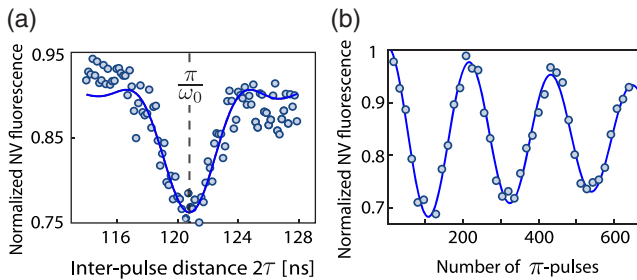


FIG. 2. Ancilla-assisted transverse field magnetometry. (a) CPMG magnetometry signal at $\Delta = 113$ MHz as a function of interpulse distance 2τ . We used quantum interpolation [50] to precisely sample the ^{14}N resonance peak. (b) Fixing the pulse distance at $2\tau = \pi/\omega_0$ and sweeping the number of π pulses we can extract the transverse field strength from the oscillation frequency [solid lines: fit to Eq. (5)].

be shorter than in the absence of a transverse field. Just as T_2^* is ultimately limited by longitudinal dc noise, T_2 in the frequency-up-conversion method is ultimately limited by the transverse dc noise. We consider the worst case scenario where the dc field to be measured introduces additional noise, which dominates other noise sources. More precisely, we consider a field $\vec{B} + \vec{\delta}$, where $\vec{\delta}$ is a stochastic, wide-sense static contribution with zero mean and auto-correlation function for each Cartesian component

$$\langle \delta(t_1)\delta(t_2) \rangle = D^2 \exp(-|t_1 - t_2|/\tau_c),$$

where D describes the variance of the noise and τ_c its correlation time. We calculate the coherence times $T_2(\gamma_X)$ and T_2^* (assuming the same noise strength in both the Z and transverse direction) using the stochastic Liouville formalism and cumulant expansion [20]. We consider two regimes of interest. When τ_c is short, we obtain

$$T_2^* = \frac{1}{\gamma_e^2 D^2 \tau_c}, \quad T_2 = \frac{1}{\gamma_X^2 D^2 \tau_c},$$

while when τ_c is long compared to the sensing time

$$T_2^* = \frac{\sqrt{2}}{\gamma_e D}, \quad T_2 = \frac{\pi}{\sqrt{2}\gamma_X D}.$$

In both cases we see that when considering the resulting sensitivity, there is a tradeoff between γ_X and $T_2(\gamma_X)$, since increasing the effective coupling also leads to shorter coherence times. Still, the sensitivity to the transverse field is now on the same order of the Ramsey sensitivity to Z field, thus much better than without the up-conversion scheme. An intuitive way to understand the dependence of T_2 on γ_X is to consider that the coupling with the nuclear spin inserts the transverse field noise into the NV sensor. This is to be expected since, in this case, transverse field noise masquerades as the signal to be measured, and there is no way to distinguish between them. Still, frequency up-conversion and quantum lock-in detection allows one to suppress Z-field noise, which is typically the dominant source of sensor noise. Potentially better scaling of the T_2 coherence time could be obtained if the main source of noise is not isotropic or it is not centered around zero frequency, as the power density spectrum will be up-converted to a frequency outside the filter bandpass of the DD sequence [13,54]. Indeed, in our experiments we obtain a longer coherence time than predicted from the worst-case scenario discussed here.

Experimental sensitivity.—We characterized the sensitivity by varying the intensity of an external static magnetic field created through a voltage source [20] close to diamond surface. The field strength is proportional to the voltage, i.e., $B_Z = \alpha V$ and $B_X = \beta V$. We calibrated both components separately [20]. In Fig. 3, we compare the signal

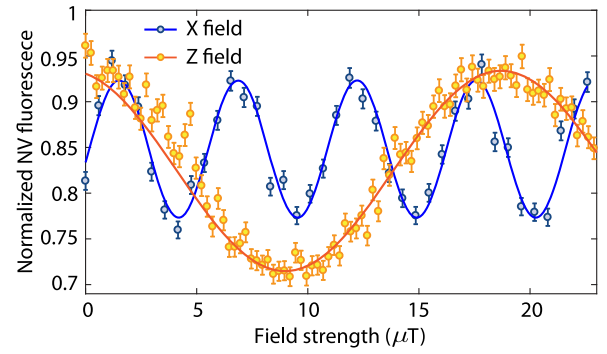


FIG. 3. Sensitivity characterization. Ramsey and CPMG magnetometry as a function of the Z- (yellow) and X-field (blue) strengths, respectively. Each blue data point corresponds to the peak as in Fig. 2(a). The Z field is measured at $\Delta = 104.6$ MHz (987.6 G) with Ramsey interrogation time $t = 2 \mu\text{s}$, which is close to the optimal time. The X field is measured at $\Delta = 18.1$ MHz (1018.5G) with 240 π pulses (total interrogation time $t = 31.2 \mu\text{s}$, slightly longer than the optimal time). To work within the validity of the rotating wave approximation, we used 100 ns long π pulses. Error bars are due to photon shot noise and collection inefficiency.

change of CPMG (blue curve) and Ramsey (yellow curve) when varying the field amplitude (either transverse or longitudinal component). CPMG interpulse spacing is fixed at the ^{14}N resonance condition. The oscillations in Fig. 3 follow Eqs. (5) and (2), respectively. From the data, the sensitivity can be extracted using the oscillation frequency, contrast, uncertainty, the total interrogation time, and dead time $t_d = 1.3 \mu\text{s}$. The measured sensitivities for the two methods were obtained to be

$$\begin{aligned} \eta_Z &= 0.42 \pm 0.02 \mu\text{T}/\sqrt{\text{Hz}}, \\ \eta_X &= 0.56 \pm 0.05 \mu\text{T}/\sqrt{\text{Hz}}, \end{aligned} \quad (7)$$

demonstrating experimentally that our method allows access to comparable sensitivities for both longitudinal and transverse components of the magnetic field, opening the path to nanoscale vector magnetometry.

We note that the faster oscillations (and lower amplitude) for transverse field sensing in Fig. 3 are on account of the longer interrogation time. In these experiments, the Ramsey coherence time T_2^* was $4.9 \mu\text{s}$, while the CPMG coherence time T_2 at ^{14}N frequency was $47 \mu\text{s}$. The coherence time T_2 measured by spin echo, on the other hand, was $240 \mu\text{s}$, indicating that the coherence time, and thus the sensitivity, is limited both by pulse errors [20] and by static noise that is up-converted to the ^{14}N frequency.

Discussion and outlook.—We have demonstrated a new modality for high sensitivity vector magnetometry that combines conventional Z-field sensing via Ramsey interferometry with transverse field sensing by quantum lock-in detection, which is enabled by frequency up-conversion

mediated by an ancillary nuclear spin. In particular, our method allows measuring the transverse field with a much better sensitivity than otherwise obtained by standard Ramsey techniques.

Our scheme presents advantages over other proposals for vector magnetometry. A first method exploits the 4 different orientations of an ensemble of NV centers along the diamond crystallographic axes [55–57]. Using spin ensembles, however, degrades the spatial resolution, forgoing the atomic-scale resolution of single defect protocols. Using a defect with a larger spin, such as V_{Si} in 4H-SiC (spin 3/2) enables vector magnetometry using a single defect [58,59], at the cost of more complex control. However, the sensitivity of a single V_{Si} magnetometer in SiC is not as good as a single NV center in diamond.

The sensitivity to transverse fields could be further improved beyond the Ramsey sensitivity, to deliver a dc-magnetic field sensor beyond the T_2^* limit. First, as the interrogation time is long compared to Ramsey sensing, transverse field sensing could benefit from advanced readout techniques, such as charge conversion sensing [60,61]. As these methods require long readout time, they are most beneficial in improving the sensitivity only when the interrogation time is also as long. Details about the effects of dead time in the calculation of sensitivity can be found in Ref. [20].

In addition, in our calculation and experiment we considered the worst case scenario where the coherence, and thus the sensitivity, is limited by the up-converted noise introduced by the signal itself (as well as by pulse errors). In particular, we assumed an isotropic, classical dc noise as the main source of decoherence, affecting in a similar way Ramsey interferometry and the up-conversion DD scheme [20]. If the main source of decoherence is different, we could achieve a better scaling of T_2 with γ_X , yielding a better sensitivity. For example, a quantum bath, arising, e.g., from nuclear spins in the diamond, is not expected to undergo a similar frequency up-conversion, and thus it could yield long coherence times in the DD scheme. Our transverse dc field sensing scheme could be further extended by using different nuclear spins (such as ^{13}C with stronger hyperfine couplings) or even other defects in diamond or SiC. As detailed in Ref. [20], if pulse errors become a limitation, the scheme is compatible with continuous driving decoupling [62,63]. Furthermore, it could be extended to measure low-frequency ac signals, that might be difficult to detect via standard DD sensing: by alternating (*maytagging*) the applied longitudinal magnetic field between two values that reverse the sign of Δ , only signals with frequency equal to the maytagging frequency are detected.

We finally remark that although we focused on magnetic field sensing, the same ideas could be applied to sensing of rotations, pressure, electric fields, and the shear component of strain tensor [20,64]. We thus anticipate applications of

our sensing technique in many areas of materials science, biology, and condensed matter physics, where vector sensing of static field can reveal fundamental properties of the target system.

We gratefully acknowledge discussions with J. Barry, S. Bhave, U. Bissbort, D. Glenn, J.-C. Jaskula, F. Jelezko, L. Marseglia, L. McGuinness, P. Neumann, K. Saha, V. Vuletic, R. Walsworth, and J. Wrachtrup. This work was supported in part by the NSF CUA PHY1734011 and the U.S. Army Research Office Grants No. W911NF-11-1-0400 and No. W911NF-15-1-0548.

*These authors contributed equally to this work.

†pcappell@mit.edu

- [1] J. R. Maze *et al.*, *Nature (London)* **455**, 644 (2008).
- [2] G. Balasubramanian, I. Y. Chan, R. Kolesov, M. Al-Hmoud, J. Tisler, C. Shin, C. Kim, A. Wojcik, P. R. Hemmer, A. Krueger, T. Hanke, A. Leitenstorfer, R. Bratschitsch, F. Jelezko, and J. Wrachtrup, *Nature (London)* **455**, 648 (2008).
- [3] C. L. Degen, F. Reinhard, and P. Cappellaro, *Rev. Mod. Phys.* **89**, 035002 (2017).
- [4] J. Wikswo, J. Barach, and J. Freeman, *Science* **208**, 53 (1980).
- [5] J. F. Barry, M. J. Turner, J. M. Schloss, D. R. Glenn, Y. Song, M. D. Lukin, H. Park, and R. L. Walsworth, *Proc. Natl. Acad. Sci. U.S.A.* **113**, 14133 (2016).
- [6] K. Jensen, R. Budvytyte, R. A. Thomas, T. Wang, A. M. Fuchs, M. V. Balabas, G. Vasilakis, L. D. Mosgaard, H. C. Stærkind, J. H. Müller, T. Heimburg, S.-P. Olesen, and E. S. Polzik, *Sci. Rep.* **6**, 29638 (2016).
- [7] B. Dellabetta, T. L. Hughes, M. J. Gilbert, and B. L. Lev, *Phys. Rev. B* **85**, 205442 (2012).
- [8] E. M. Spanton, K. C. Nowack, L. Du, G. Sullivan, R.-R. Du, and K. A. Moler, *Phys. Rev. Lett.* **113**, 026804 (2014).
- [9] I. Gross, W. Akhtar, V. Garcia, L. J. Martinez, S. Chouaieb, K. Garcia, C. Carretero, A. Barthelemy, P. Appel, P. Maletinsky, J. V. Kim, J. Y. Chauleau, N. Jaouen, M. Viret, M. Bibes, S. Fusil, and V. Jacques, *Nature (London)* **549**, 252 (2017).
- [10] N. F. Ramsey, *Phys. Rev.* **78**, 695 (1950).
- [11] F. Casola, T. van der Sar, and A. Yacoby, *Nat. Rev. Mater.* **3**, 17088 (2018).
- [12] S. Kotler, N. Akerman, Y. Glickman, A. Keselman, and R. Ozeri, *Nature (London)* **473**, 61 (2011).
- [13] M. J. Biercuk, A. C. Doherty, and H. Uys, *J. Phys. B* **44**, 154002 (2011).
- [14] J. T. Hill, A. H. Safavi-Naeini, J. Chan, and O. Painter, *Nat. Commun.* **3**, 1196 (2012).
- [15] M. T. Rakher, L. Ma, O. Slattery, X. Tang, and K. Srinivasan, *Nat. Photonics* **4**, 786 (2010).
- [16] H. Y. Carr and E. M. Purcell, *Phys. Rev.* **94**, 630 (1954).
- [17] S. Meiboom and D. Gill, *Rev. Sci. Instrum.* **29**, 688 (1958).
- [18] T. Gullion, D. B. Baker, and M. S. Conradi, *J. Magn. Reson.* **89**, 479 (1990).
- [19] We consider the $m_I = 0, +1$ levels only as the ^{14}N is polarized at the fields considered.

- [20] See Supplemental Material at <http://link.aps.org/supplemental/10.1103/PhysRevLett.122.100501> for calculations of sensor parameters, effect of experimental imperfections, effect of long dead time, application to strain sensing, and description of sensing setup, etc., which includes Refs. [21–48].
- [21] M. A. Nielsen, *Phys. Lett. A* **303**, 249 (2002).
- [22] M. Hirose and P. Cappellaro, *Quantum Inf. Process.* **17**, 88 (2018).
- [23] G. D. Fuchs, V. V. Dobrovitski, D. M. Toyli, F. J. Heremans, and D. D. Awschalom, *Science* **326**, 1520 (2009).
- [24] J. Scheuer, X. Kong, R. S. Said, J. Chen, A. Kurz, L. Marseglia, J. Du, P. R. Hemmer, S. Montangero, T. Calarco, B. Naydenov, and F. Jelezko, *New J. Phys.* **16**, 093022 (2014).
- [25] T. W. Kornack, S. J. Smullin, S.-K. Lee, and M. V. Romalis, *Appl. Phys. Lett.* **90**, 223501 (2007).
- [26] P. London, J. Scheuer, J.-M. Cai, I. Schwarz, A. Retzker, M. B. Plenio, M. Katagiri, T. Teraji, S. Koizumi, J. Isoya, R. Fischer, L. P. McGuinness, B. Naydenov, and F. Jelezko, *Phys. Rev. Lett.* **111**, 067601 (2013).
- [27] C. Belthangady, N. Bar-Gill, L. M. Pham, K. Arai, D. Le Sage, P. Cappellaro, and R. L. Walsworth, *Phys. Rev. Lett.* **110**, 157601 (2013).
- [28] S. R. Hartmann and E. L. Hahn, *Phys. Rev.* **128**, 2042 (1962).
- [29] A. Pines, M. G. Gibby, and J. S. Waugh, *J. Chem. Phys.* **59**, 569 (1973).
- [30] H. Fedder, F. Dolde, F. Rempp, T. Wolf, P. Hemmer, F. Jelezko, and J. Wrachtrup, *Appl. Phys. B* **102**, 497 (2011).
- [31] A. M. Souza, G. A. Álvarez, and D. Suter, *Phys. Rev. Lett.* **106**, 240501 (2011).
- [32] J. R. Schrieffer and P. A. Wolff, *Phys. Rev.* **149**, 491 (1966).
- [33] S. Bravyi, D. DiVincenzo, and D. Loss, *Ann. Phys. (Amsterdam)* **326**, 2793 (2011).
- [34] E. R. MacQuarrie, T. A. Gosavi, N. R. Jungwirth, S. A. Bhave, and G. D. Fuchs, *Phys. Rev. Lett.* **111**, 227602 (2013).
- [35] M. W. Doherty, F. Dolde, H. Fedder, F. Jelezko, J. Wrachtrup, N. B. Manson, and L. C. L. Hollenberg, *Phys. Rev. B* **85**, 205203 (2012).
- [36] E. R. MacQuarrie, T. A. Gosavi, S. A. Bhave, and G. D. Fuchs, *Phys. Rev. B* **92**, 224419 (2015).
- [37] M. S. J. Barson, P. Peddibhotla, P. Ovarthaiyapong, K. Ganesan, R. L. Taylor, M. Gebert, Z. Mielens, B. Koslowski, D. A. Simpson, L. P. McGuinness *et al.*, *Nano Lett.* **17**, 1496 (2017).
- [38] D. A. Golter, T. Oo, M. Amezcua, K. A. Stewart, and H. Wang, *Phys. Rev. Lett.* **116**, 143602 (2016).
- [39] S. Meesala, Y.-I. Sohn, H. A. Atikian, S. Kim, M. J. Burek, J. T. Choy, and M. Loncar, *Phys. Rev. Applied* **5**, 034010 (2016).
- [40] J. Teissier, A. Barfuss, P. Appel, E. Neu, and P. Maletinsky, *Phys. Rev. Lett.* **113**, 020503 (2014).
- [41] A. Barfuss, J. Teissier, E. Neu, A. Nunnenkamp, and P. Maletinsky, *Nat. Phys.* **11**, 820 (2015).
- [42] P. Ovarthaiyapong, K. W. Lee, B. A. Myers, and A. C. B. Jayich, *Nat. Commun.* **5**, 4429 (2014).
- [43] R. Kubo, *J. Math. Phys. (N.Y.)* **4**, 174 (1963).
- [44] T. Unden, P. Balasubramanian, D. Louzon, Y. Vinkler, M. B. Plenio, M. Markham, D. Twitchen, A. Stacey, I. Lovchinsky, A. O. Sushkov, M. D. Lukin, A. Retzker, B. Naydenov, L. P. McGuinness, and F. Jelezko, *Phys. Rev. Lett.* **116**, 230502 (2016).
- [45] J.-P. Tetienne, L. Rondin, P. Spinicelli, M. Chipaux, T. Debuisschert, J.-F. Roch, and V. Jacques, *New J. Phys.* **14**, 103033 (2012).
- [46] T. van der Sar, F. Casola, R. Walsworth, and A. Yacoby, *Nat. Commun.* **6**, 8886 (2015).
- [47] A. Wickenbrock, H. Zheng, L. Bougas, N. Leefer, S. Afach, A. Jarmola, V. M. Acosta, and D. Budker, *Appl. Phys. Lett.* **109**, 053505 (2016).
- [48] V. Jacques, P. Neumann, J. Beck, M. Markham, D. Twitchen, J. Meijer, F. Kaiser, G. Balasubramanian, F. Jelezko, and J. Wrachtrup, *Phys. Rev. Lett.* **102**, 057403 (2009).
- [49] M. Chen, M. Hirose, and P. Cappellaro, *Phys. Rev. B* **92**, 020101 (2015).
- [50] A. Ajoy, Y.-X. Liu, K. Saha, L. Marseglia, J.-C. Jaskula, U. Bissbort, and P. Cappellaro, *Proc. Natl. Acad. Sci. U.S.A.* **114**, 2149 (2017).
- [51] L. Childress, M. V. Gurudev Dutt, J. M. Taylor, A. S. Zibrov, F. Jelezko, J. Wrachtrup, P. R. Hemmer, and M. D. Lukin, *Science* **314**, 281 (2006).
- [52] J. H. Shim, I. Niemeyer, J. Zhang, and D. Suter, *Phys. Rev. A* **87**, 012301 (2013).
- [53] W. M. Itano, J. C. Bergquist, J. J. Bollinger, J. M. Gilligan, D. J. Heinzen, F. L. Moore, M. G. Raizen, and D. J. Wineland, *Phys. Rev. A* **47**, 3554 (1993).
- [54] A. A. Wood, E. Lilette, Y. Y. Fein, N. Tomek, L. P. McGuinness, L. C. L. Hollenberg, R. E. Scholten, and A. M. Martin, *Sci. Adv.* **4**, eaar7691 (2018).
- [55] S. Steinert, F. Dolde, P. Neumann, A. Aird, B. Naydenov, G. Balasubramanian, F. Jelezko, and J. Wrachtrup, *Rev. Sci. Instrum.* **81**, 043705 (2010).
- [56] H. Clevenson, L. M. Pham, C. Teale, K. Johnson, D. Englund, and D. Braje, *Appl. Phys. Lett.* **112**, 252406 (2018).
- [57] J. M. Schloss, J. F. Barry, M. J. Turner, and R. L. Walsworth, *Phys. Rev. Applied* **10**, 034044 (2018).
- [58] S.-Y. Lee, M. Niethammer, and J. Wrachtrup, *Phys. Rev. B* **92**, 115201 (2015).
- [59] M. Niethammer, M. Widmann, S.-Y. Lee, P. Stenberg, O. Kordina, T. Ohshima, N. T. Son, E. Janzén, and J. Wrachtrup, *Phys. Rev. Applied* **6**, 034001 (2016).
- [60] B. J. Shields, Q. P. Unterreithmeier, N. P. de Leon, H. Park, and M. D. Lukin, *Phys. Rev. Lett.* **114**, 136402 (2015).
- [61] J.-C. Jaskula, B. J. Shields, E. Bauch, M. D. Lukin, A. S. Trifonov, and R. L. Walsworth, [arXiv:1711.02023](https://arxiv.org/abs/1711.02023).
- [62] M. Hirose, C. D. Aiello, and P. Cappellaro, *Phys. Rev. A* **86**, 062320 (2012).
- [63] M. Loretz, T. Rosskopf, and C. L. Degen, *Phys. Rev. Lett.* **110**, 017602 (2013).
- [64] P. Udvarhelyi, V. O. Shkolnikov, A. Gali, G. Burkard, and A. Pályi, *Phys. Rev. B* **98**, 075201 (2018).